

HIGH ASPECT RATIO WING WITH CURVED PLANFORM: CFD AND FE ANALYSES

M. R. Chiarelli*, M. Cagnoni*, M. Ciabattari*, M. De Biasio*, A. Massai**
 *Department of Aerospace Engineering – University of Pisa, Italy
 **AM Engineering, Firenze, Italy

Keywords: *high aspect ratio wing, curved planform, wave drag, drag reduction*

Abstract

Modern configurations of aircraft deal with a high performance design of lifting systems especially oriented to reduction of weight, aerodynamic drag and fuel consumption. The paper shows preliminary results of aerodynamic and structural analyses of a high aspect ratio wing with curved planform, carried out at the Department of Aerospace Engineering of the University of Pisa. In transonic flight condition (high subsonic), for curved planform wing, the wave drag effects are significantly reduced. A numerical comparison, carried out using the FLUENT[®] code, between curved and traditional swept wing, both designed with the same supercritical airfoil, shows a drag coefficient reduction of 4% and more for asymptotic Mach numbers greater than 0.85. The B787 aircraft's wing planform has been assumed as reference geometry to carry out the numerical analyses. The curved planform configuration also improves the aeroelastic behaviour of the wing: some preliminary results obtained using the NASTRAN[®] code are summarized in the paper.

1 Introduction

The cruise speed of commercial jet-planes is actually fixed on the basis of the best compromise between flying times and fuel consumption, under the constraints imposed by structure resistance and maximum aircraft's productivity requirements.

Under transonic conditions, a portion of the energy of the fluid flow, across the shock wave, is transformed into heat because of dissipative effects associated to the aerodynamic field, the pressure suddenly increases and boundary layer

separation can occur.

These phenomena produce the so called “Wave Drag”, which is an important percentage of the total aerodynamic drag of the aircraft.

Beyond producing an increase of the aerodynamic drag of the aircraft, shock waves formation can lead to non stationary phenomena which can modify the performances of the lifting surfaces, and can even produce dangerous oscillations of the wing.

The more intense the shock waves on wing surface, the more important all the phenomena here above described.

It is well known that a method to reduce the effect of a shock wave, which develops along a wing in the transonic regime, can be to increase the swept angle of the leading edge. Modern aircrafts have high value of this angle (Boeing B787 and Airbus A350 XWB are last important examples).

In order to reduce the shock wave effects, a high aspect ratio wing with a curved planform has been preliminary designed at the Department of Aerospace Engineering of Pisa University [1], [2], [4]. The curved wing is characterised by having a gradually increasing swept angle of the leading edge along the span wise direction.

In the technical literature the authors have found few examples of application of wings with curved or partially curved planform: some of these examples can be found in [5], [6], [7]. Moreover, in the cited works, the strong effect of planform shape on the pressure distribution along the wing in the transonic regime has not been explicitly studied. In [5] a glider with curved wings is treated; in [6] subsonic tests have been executed on elliptical and descent wing (a curved wing) to compare drag and lift

characteristics of the two wings; in [7] the geometry of a wing tip extension with variable dihedral and swept is discussed and effects on “*a significant reduction of the induced drag and an improvement of the wave drag*” are highlighted but not quantified.

At the Department of Aerospace Engineering of Pisa, during a first campaign of numerical analyses, it was immediately evident that an important drag reduction can be obtained by adopting a curved shape to design the leading edge of the high aspect ratio wing [1].

Further detailed comparative analyses have shown that, assuming the same supercritical airfoil to construct numerical models of a traditional swept wing and a wing with a curved planform, a reduction of 4% in the drag coefficient can be reached for a Mach number equal to 0.85, i.e. in a full transonic regime [2], [4]. Moreover, preliminary aeroelastic analyses have shown a good behaviour of the Curved Wing, compared with a Swept Wing, due to favourable effects of structural interactions between torsion and bending [3], [4].

A sketch of the reference geometry of the examined half wing is shown in Fig. 1. In Fig. 2 the selected supercritical airfoil, used in the half wing modelling, is represented [8]. The main geometrical parameters of the reference wing are summarized in Table 1. In all the mentioned references and in the present paper, swept and curved wings have the same aspect ratio.

Fig. 3 shows the geometry assumed to evaluate the effects that the fuselage has on pressure and velocity distribution on the upper and lower surfaces of the two different wings.

The shape of the leading edge of the curved wing has been defined by fixing the values of the slope at root and tip sections and by assuming a second order law in the span direction.

Both in the swept and in the curved wing configurations the geometry of the airfoil, used to create the CAD models, has been introduced in the X-Y reference plane shown in Fig. 3 and Fig. 4. In this way, the selected supercritical airfoil lies on planes parallel to the longitudinal plane of the aircraft half model.

Fig. 4 shows the position of some reference planes along the wing span: for the airfoils lying

on these reference planes (aligned with the stream direction), graphs of the pressure coefficient and of the local Mach values will be shown and discussed in the following paragraphs.

2 CFD Analyses of the Wing-Body Models

2.1 Overall Data of Numerical Models

Two wing-body models have been constructed starting from a CAD archive and transferring the geometrical information to the CFD pre-processor GAMBIT[®]. As done in previous works [2] and [4], the study of the present wing-body geometries, with a swept and a curved wing, has been carried out according to the sketch shown in Fig. 3: i.e. at the root section the leading edge of the curved wing has the same slope of the leading edge of the reference swept wing.

In order to take into account the viscosity effects, a turbulent and viscous flow condition have been assumed during CFD analyses. A standard K- ϵ model (2 equations) has been used to describe turbulence, and unstructured grids composed of about 2,300,000 tetrahedral cells have been built. A sketch of the half wing-body CFD model is shown in Fig. 5 and Fig. 6. The dimensions of the grid volume are detailed in Table 2; the grid and model reference frame is represented in Fig. 3 and Fig. 4.

Pressure far field boundary condition has been fixed for all the free faces of the grid volume, and the symmetry boundary condition has been assigned to the fuselage longitudinal plane.

2.2 Reference Conditions of CFD Analyses

The objective of the present CFD analysis is a comparative study of two different lifting systems and to draw the CD-Mach curves for the two configurations under the following hypotheses:

- (a) Altitude = 10,000 m (CL = 0.4);
- (b) Altitude = 10,000 m (Lift = 2,069,000 N).

In view of the previous objective, the intent of the authors was not to evaluate accurately the drag coefficient and its absolute values for the examined configurations, but it was to fix a numerical comparison between two wing-body models, from the aerodynamic point of view, in the transonic regime.

To execute this comparison the following Mach numbers have been chosen: 0.70, 0.80, 0.85, 0.875, 0.90. Drag polar curves have been drawn interpolating the calculated data and finally an estimation of the drag coefficient per cent reduction has been obtained.

Standard air parameters have been assumed for all the analyses. Values of Mach number greater than 0.90 were not investigated during the present research and will be treated in subsequent activities.

2.3 Results of CFD Analyses

In the present study the following reference values have been assumed: altitude $H=10,000$ m, $Mach=0.85$ and $CL=0.4$. For these values of *altitude*, *Mach number* and *lift coefficient* contour graphs of C_p (pressure coefficient) and Local Mach Values have been obtained for the two compared wing-body configurations: Swept Wing and Curved Wing. Contour graphs are represented in the figures from Fig. 7 to Fig. 14.

The shock wave fronts and their different shapes are outlined in the figures relevant to the upper surface of the wings. The supersonic bubbles take place only on the upper surface of the two wings while a fully subsonic flow develops through their lower surface.

Graphs of the pressure coefficients and the local Mach distribution on upper and lower surfaces (for the airfoils lying on the control sections defined in Fig. 4), are shown from Fig. 15 to Fig. 24. Full symbols have been used for the curved wing data, while empty symbols have been used for the swept wing data.

Position and intensity of the shock waves, obtained for the two different configurations, are easily available from these figures. In the external zone (toward the wing tip) of the wing, the wave front develops between 60% and 70% of chord length for S-Wing while in the case of C-Wing the wave front progressively moves

back towards the wing leading edge. From the same figures the width of supersonic bubbles can also be estimated and compared. In order to highlight the differences, the Mach number's contours (section profiles $Z/B=0.7$) of the Curved Wing and Swept Wing are shown in Fig. 25 and in Fig. 26 respectively. The evident result is that the supersonic region in the Swept Wing configuration is greater than in the Curved Wing, and the shape of its boundary (the so called Sonic Line) is different especially close to the upper surface of the wing profile. Strong three-dimensional effects arise in this case. Moreover the intensity of the pressure gradient across the shock wave is lower for the C-Wing (Fig. 16 to Fig. 19): this fact is favourable to delay the flow separation.

Collecting all the CFD results, drag polar curves have been calculated and plotted in Fig. 27, Fig. 28, Fig. 29 and Fig. 30. Interpolating the calculated data, analytical expressions, highlighted in the same figures, has been obtained. Finally, the CD -Mach curves have been drawn: these curves are shown in Fig. 31 (with $CL=0.4$) and Fig. 32 (at constant Lift and variable CL). In these figures the favourable aerodynamic behaviour of curved wing configuration is shown, that is, in the transonic regime a considerable reduction of drag coefficient can be achieved.

3 FE Analysis of the Wings

3.1 FE Models and Flutter Analysis Results

In order to perform a preliminary check of the aeroelastic behaviour of the Curved Wing, finite element models of both Swept Wing and Curved Wing have been prepared and analysed.

The structural configuration of the wing boxes has been assumed similar for the two wings as shown in Fig. 33. In this study ribs were disposed along planes parallel to the fuselage longitudinal axis. The entire wing span has been modelled to take into account directly symmetrical and non symmetrical normal modes of vibration.

The structural mass of the two wings is equal to 5,000 kg; in the model also the nacelle

engine has been considered introducing a mass of 5,000 kg (two nacelles symmetrically mounted on the wing). The inertial effects of the fuselage have also been introduced in the plane of symmetry of the wing (according to Fig. 33: fuselage mass = 90,000 kg, $I_{zz} = I_{yy} = 450,000 \text{ kg m}^2$, $I_{xx} = 90,000 \text{ kg m}^2$). The fuel stored inside the wing has been simulated as a non structural mass distribution of 40,000 kg. A metallic material (aluminium alloy) has been assumed in the FE analyses [3].

The NASTRAN[®] commercial code has been used to carry out the comparative flutter analysis of the two wings. Two reference condition have been taken into account: sea level altitude and cruise altitude.

The graphs of critical curves of damping and frequency, coming out from the calculation, are summarized in Fig. 34 and Fig. 35 ([3], [4]).

In both cases, for the two type of wings, a symmetric bending-torsion normal mode (with a natural frequency of about 2 Hz) leads to the flutter instability condition. At sea level the flutter velocity calculated for the curved wing is higher than the swept wing one. At the cruise altitude condition the two wing-body configurations examined show the same value of the flutter velocity.

These preliminary results show how the high aspect ratio curved wing configuration can be developed leading also to a suitable reduction of the wing box structural weight: in fact adopting a similar structural configuration the critical flutter condition of curved wing is considerably delayed.

4 Conclusions and Future Research Activity

In the paper it has been shown that the curved planform of a high aspect ratio wing strongly influences C_p and Mach distribution along the wing span, also considering the presence of the fuselage: assuming similar flight conditions (same value of CL) the shock wave has a lower intensity on the Curved Wing, and favourable smoother distributions of C_p and local Mach number can be obtained adopting this wing geometry.

Analysing the graphs of C_p and Mach number distribution at some control section

profiles (see Fig. 15 to Fig. 24) it can be concluded that the pressure rise across the shock wave is less intense and smoother in the Curved Wing, and consequently, the interaction with the adverse pressure gradient towards the trailing edge is reduced. It can be expected that the separation of the boundary layer of the Curved Wing is delayed with respect to the Swept Wing in the transonic regime, with consequent beneficial effects on the drag.

The plant shape of the shock wave front is strongly influenced by the leading edge shape of the wing: isobar lines tend to thicken near the leading edge of the Curved Wing (compare Fig. 7 with Fig. 9 and Fig. 11 with Fig. 13).

Considering a supercritical airfoil in the numerical models of the wing, the calculated per cent reduction of the drag coefficient is about 4% for an asymptotic Mach number equal to 0.85, and it increases up to 8.5% for a Mach number equal to 0.875. In general, Curved Wing has higher values of the Mach Drag Rise (Fig. 31, Fig. 32). The reduction of the drag coefficient is much more evident looking at the available drag polar curves (Fig. 28, Fig. 29, Fig. 30).

Because of the limits of the computational resources available in developing the research, grid's refinement was not very high. This fact leads to a non optimised modelling of the boundary layer, and certainly absolute values of the drag coefficient are affected by errors, but within the limits of a comparative study the results obtained confirm that the effects of the curved planform configuration of a wing is not negligible from the aerodynamic point of view in the transonic regime.

From the FE preliminary analysis, carried out with the same structural configuration of the two wings under comparison, it can be said that the curved wing shows a very good behaviour against flutter instabilities. The interaction between bending and torsion is favourable with respect to traditional Swept Wing and, as result, the flutter velocity of the Curved Wing configuration is higher than the flutter velocity of the Swept Wing at the sea level, while similar values are obtained for an altitude of 10,000 m. Moreover, it must be considered that the NASTRAN[®] code does not take into account

the real instability effects connected to shock wave development and flow separation in the transonic regime; for this reason, the present preliminary aeroelastic results can be assumed to be conservative due to the lower intensity of the shock waves that develop on the wings with a curved planform.

The curved planform wing configuration studied at the Department of Aerospace Engineering of Pisa University certainly will be a subject of further and more detailed analyses.

The accuracy of CFD analyses will be improved, and a configuration with available experimental results in the literature will be taken into account. A possible candidate could be, for instance, the DLR-F6 geometry [9].

Also, low speed flight regime shall be considered in order to demonstrate a good behaviour of the Curved Wing configuration for high value of the lift coefficient. High angle of attack performances have also to be studied.

The disposition of section profiles along the wing span will be modified: a configuration with the airfoils lying on planes orthogonal to the leading edge of the wings will be examined. Moreover the effect of different shape of the leading edge curve will be taken into account.

Finally, the structural design of the wing will be more in depth investigated to better demonstrate the improvement of torsion-bending interaction in a Curved Wing box layout.

At the moment of the submission of this paper, the high aspect ratio curved wing configuration has been submitted for a national patent: Italian demand code PI2009A000079.

References

- [1] Muscolo M. *Preliminary CFD analysis of a wing with high aspect ratio and a curved planform*. First Level Degree Thesis in Aerospace Engineering, Department of Aerospace Engineering, CD-ROM n. 296, University of Pisa, Pisa, Italy, April 2008.
- [2] Cagnoni M., Ciabattari M. *Planform effects on the drag polar of high aspect ratio wings: comparison between a swept wing and a curved planform's wing*. First Level Degree Thesis in Aerospace Engineering, Department of Aerospace Engineering, CD-ROM n. 344, University of Pisa, Pisa, Italy, March 2009.
- [3] De Biasio M. *Preliminary analysis of the aeroelastic behaviour of a new conception wing*. University of Pisa, Master Degree Thesis in Aerospace Engineering, Pisa, Italy, June 2009.
- [4] Chiarelli M.R., Cagnoni M., Ciabattari M., De Biasio M., Massai A. Preliminary analysis of a high aspect ratio wing with curved planform, *CD-Rom Proceedings of the XX Congresso Nazionale AIDAA*, ISBN 978-88-904668-0-9, Milano, Italy, June 2009.
- [5] Zepf H.P. Aerodynamische Auslegung für Flugzeuger holer Streckung mit positiver Tragflügelpeilung, Pub. No. DE29621652U1, <http://ep.espacenet.com/>, 16 April 1998.
- [6] Van Dam C.P., Vijgen P.M.H.W., Holmest B.J. Experimental Investigation on the Effect of Crescent Planform on Lift and Drag, *Journal of Aircraft*, Vol. 28, No. 11, pp. 713-720, 1991.
- [7] Heller G. et alii Wing Tip Extension for a Wing, Pub. No. US2002162917A1, <http://ep.espacenet.com/>, 7 November 2002.
- [8] Harris C.D. *NASA Supercritical Airfoils, A Matrix of Family-Related Airfoils*. NASA Technical Paper 2969, Langley Research Center, Hampton, Virginia, March 1990.
- [9] Brodersen O, Stürmer A. Drag Prediction of Engine-Airframe Interference Effects Using Unstructured Navier-Stokes Calculations, *AIAA 2001-2014, 19th AIAA Applied Aerodynamics Conference*, Anaheim, California, June 2001.

5 Contact Author Email Address

The contact author email address is: chiarelli@ing.unipi.it

Copyright Statement

The authors confirm that they, and/or their company or organization, hold copyright on all of the original material included in this paper. The authors also confirm that they have obtained permission, from the copyright holder of any third party material included in this paper, to publish it as part of their paper. The authors confirm that they give permission, or have obtained permission from the copyright holder of this paper, for the publication and distribution of this paper as part of the ICAS2010 proceedings or as individual off-prints from the proceedings.

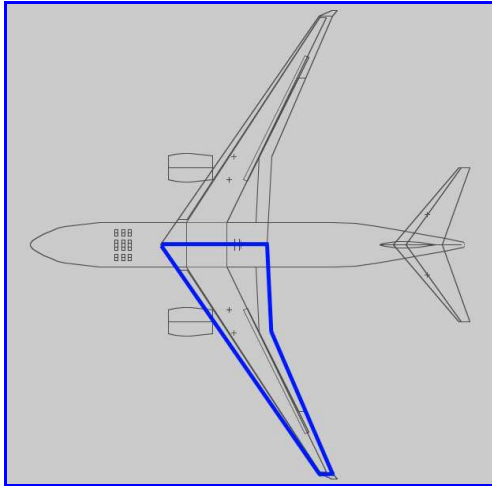


Fig. 1. Sketch of B787 aircraft configuration

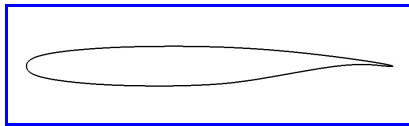


Fig. 2. 10-Percent-Thick Supercritical Airfoil SC(2)-0410 (Ref. [8])

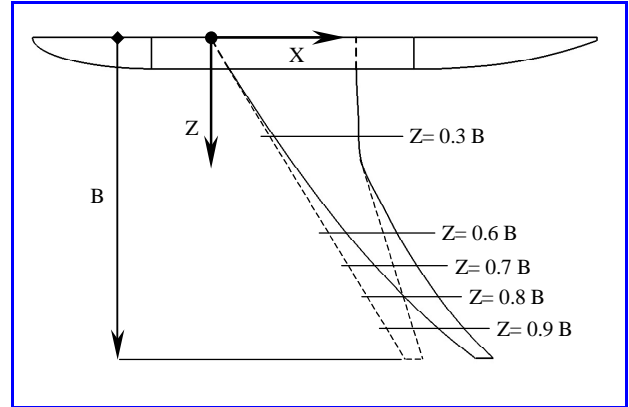


Fig. 4. Position of the control sections along the wings

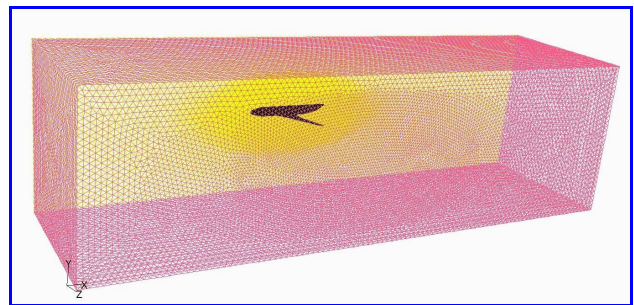


Fig. 5. Overall view of the grid used in the CFD analyses (swept wing model)

Table 1. Geometry parameters of reference swept wing

Half Wing plant surface	193 m ²
Half Wing span (B)	30 m
Swept angle (at the leading edge)	32°
Root chord	14.27 m
Kink chord	6.42 m
Tip chord	1.7 m
Aspect Ratio of wing (AR)	9.48

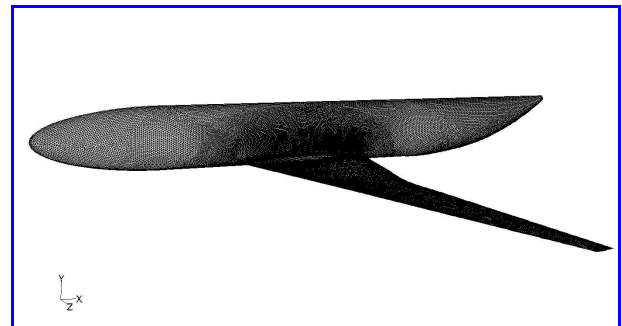


Fig. 6. View of the surface grid of the wing-body configuration (swept wing model)

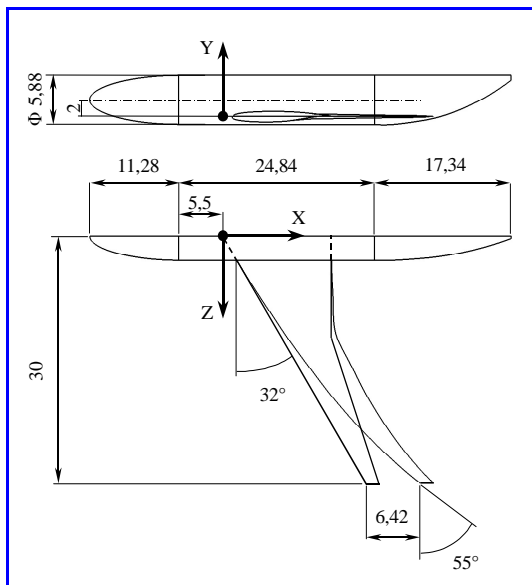


Fig. 3. Sketch of the half wing-body geometries analysed

Table 2. Dimensions of grid volume

X_min	-150 m
Y_min	-50 m
Z_min	0
X_max	200 m
Y_max	50 m
Z_max	100 m

HIGH ASPECT RATIO WING WITH CURVED PLANFORM: CFD AND FE ANALYSES

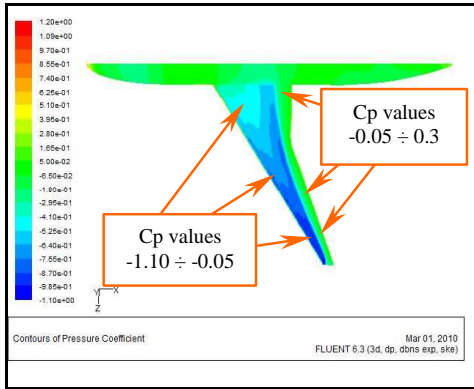


Fig. 7. S-Wing upper surface (CL=0.4, Mach=0.85)

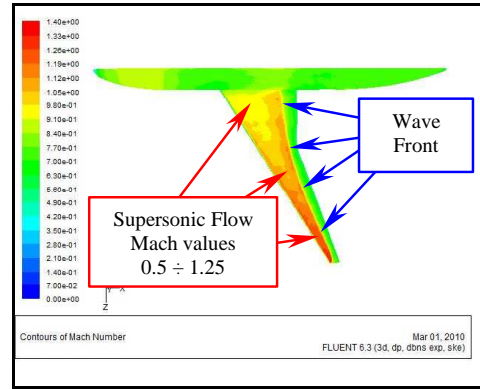


Fig. 11. S-Wing upper surface (CL=0.4, Mach=0.85)

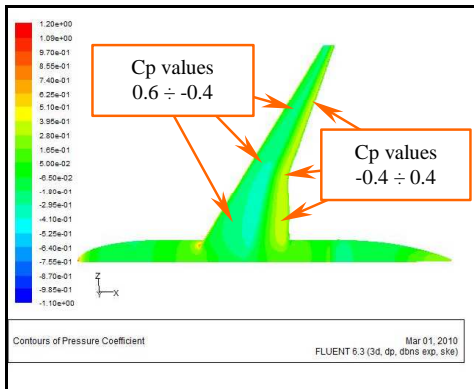


Fig. 8. S-Wing lower surface (CL=0.4, Mach=0.85)

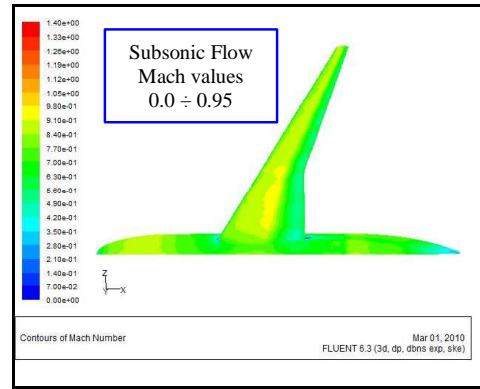


Fig. 12. S-Wing lower surface (CL=0.4, Mach=0.85)

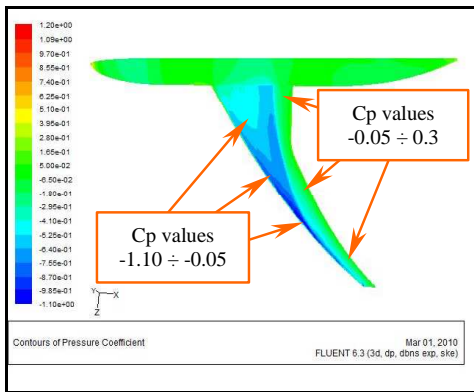


Fig. 9. C-Wing upper surface (CL=0.4, Mach=0.85)

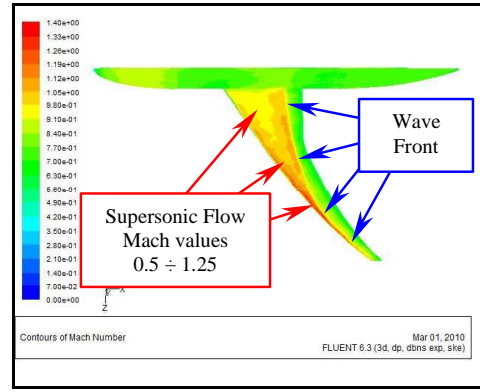


Fig. 13. C-Wing upper surface (CL=0.4, Mach=0.85)

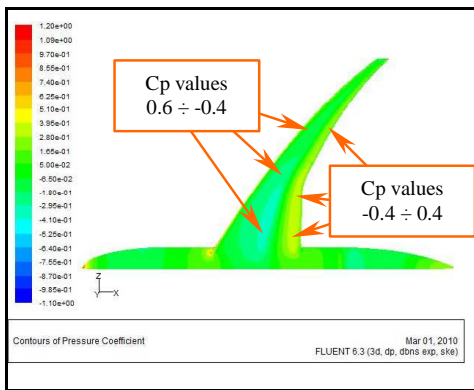


Fig. 10. C-Wing lower surface (CL=0.4, Mach=0.85)

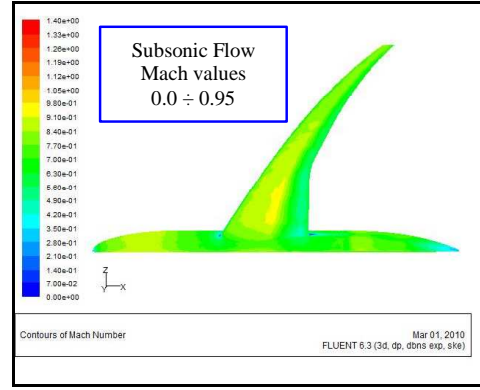


Fig. 14. C-Wing lower surface (CL=0.4, Mach=0.85)

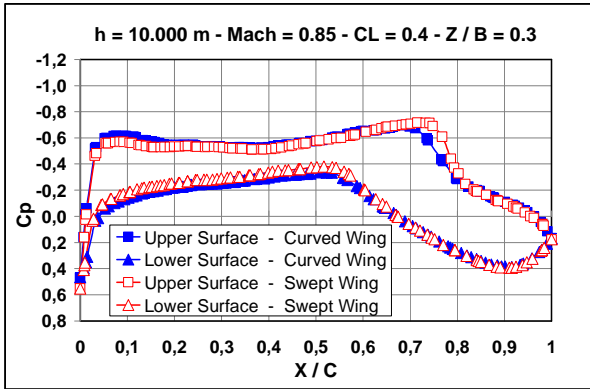


Fig. 15. Graphs of pressure coefficient (section Z/B=0.3)

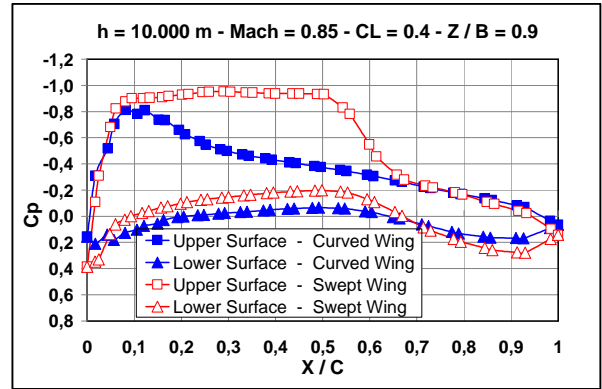


Fig. 19. Graphs of pressure coefficient (section Z/B=0.9)

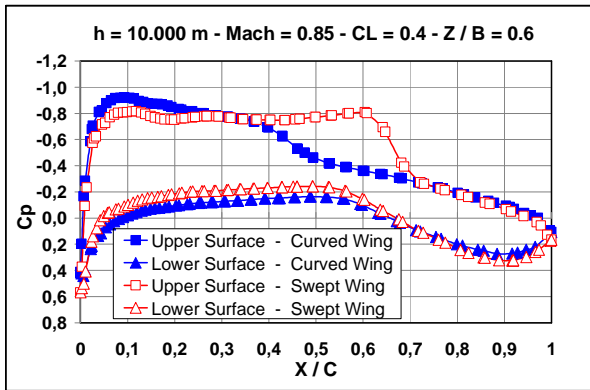


Fig. 16. Graphs of pressure coefficient (section Z/B=0.6)

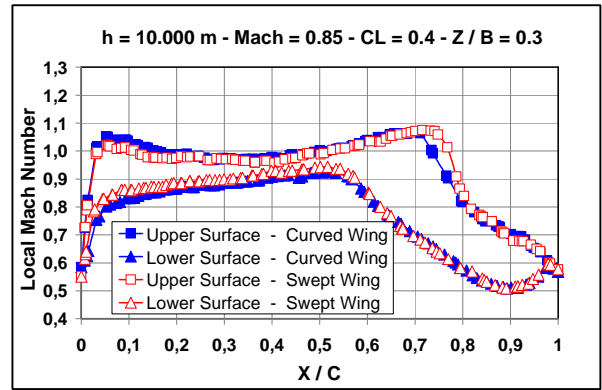


Fig. 20. Graphs of local Mach values (section Z/B=0.3)

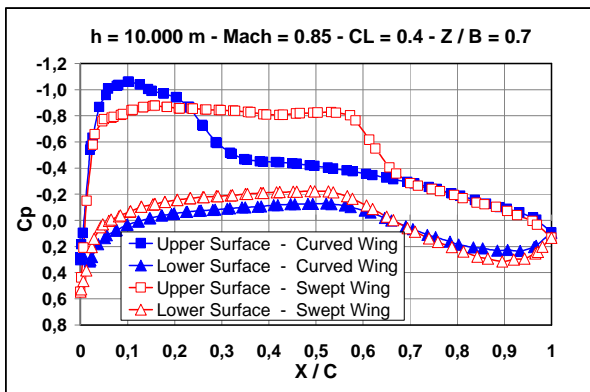


Fig. 17. Graphs of pressure coefficient (section Z/B=0.7)

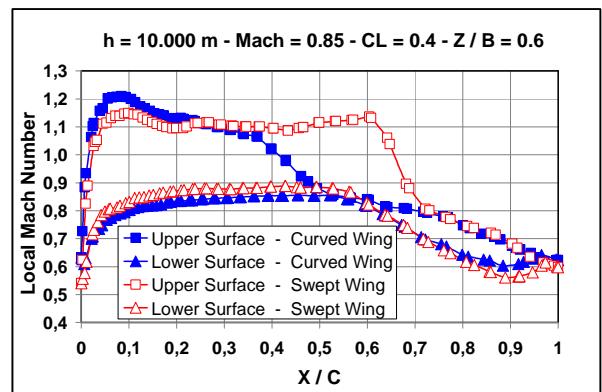


Fig. 21. Graphs of local Mach values (section Z/B=0.6)

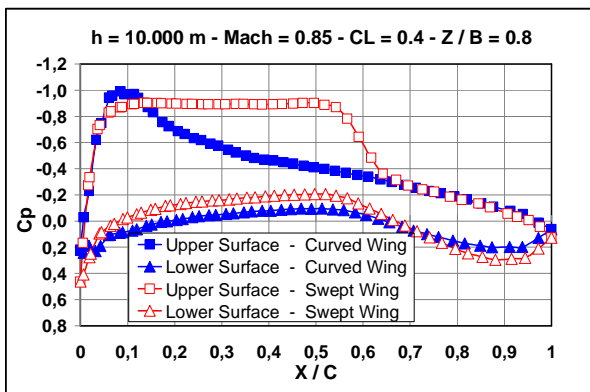


Fig. 18. Graphs of pressure coefficient (section Z/B=0.8)

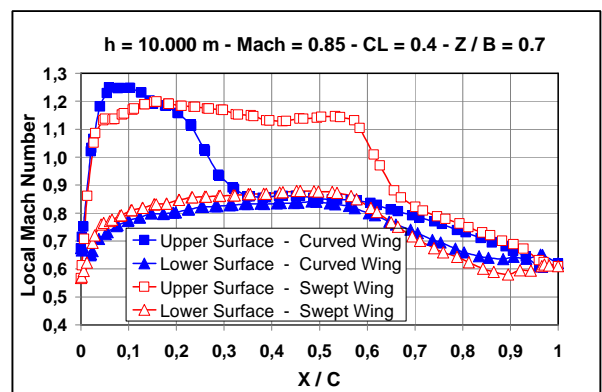


Fig. 22. Graphs of local Mach values (section Z/B=0.7)

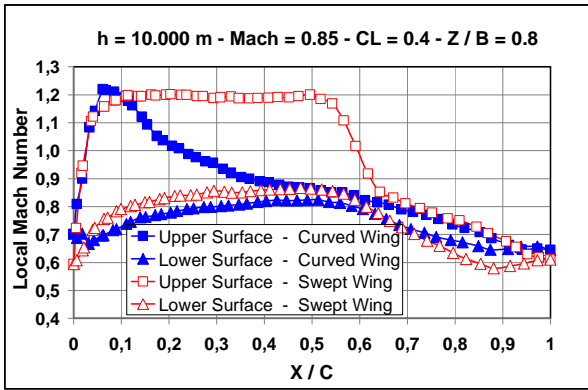


Fig. 23. Graphs of local Mach values (section Z/B=0.8)

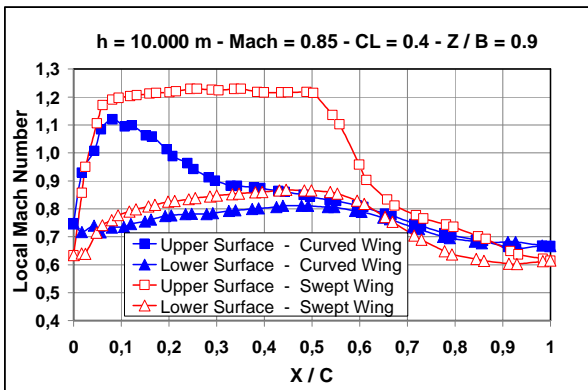


Fig. 24. Graphs of local Mach values (section Z/B=0.9)

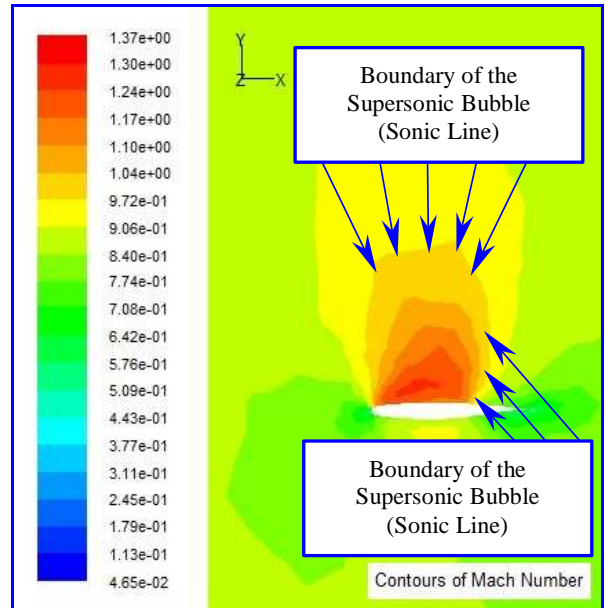


Fig. 26: S-Wing Supersonic bubble Z/B=0.7 Mach=0.85

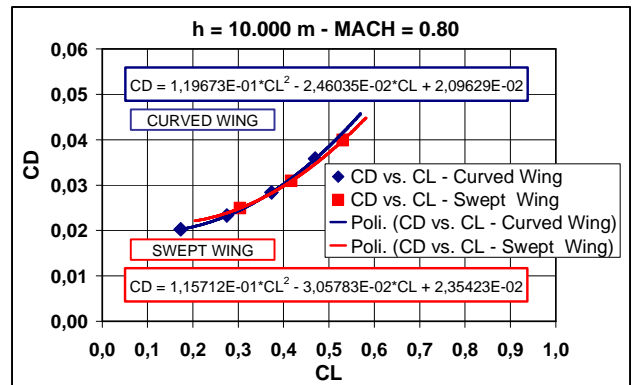


Fig. 27. Drag Polar curves (Mach=0.80)

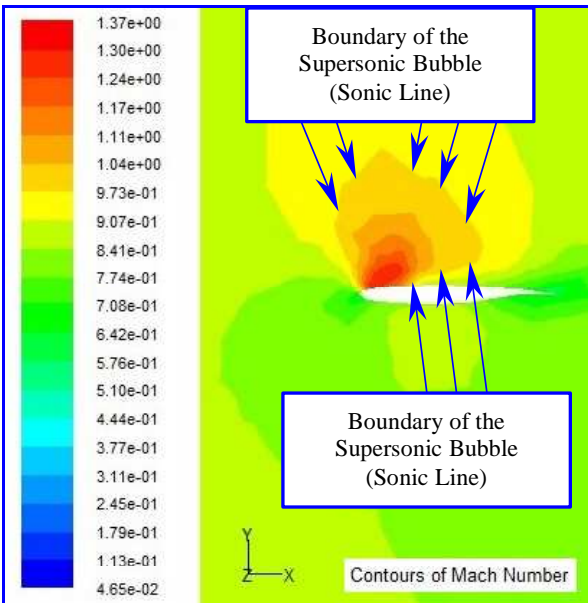


Fig. 25: C-Wing Supersonic bubble Z/B=0.7 Mach=0.85

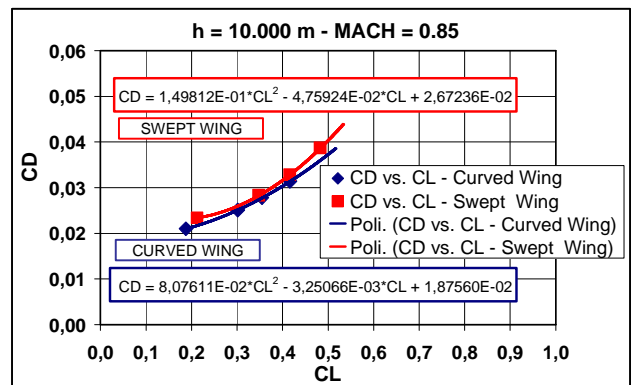


Fig. 28. Drag Polar curves (Mach=0.85)

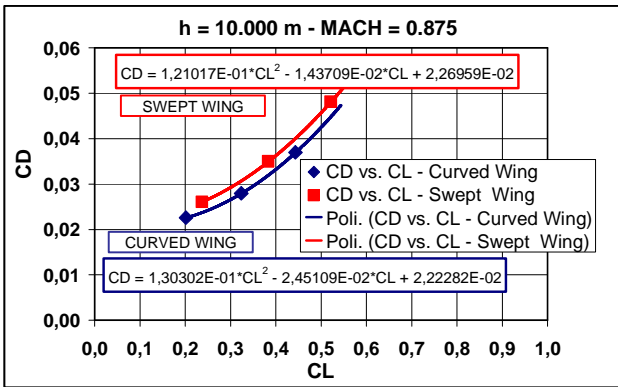


Fig. 29. Drag Polar curves (Mach=0.875)

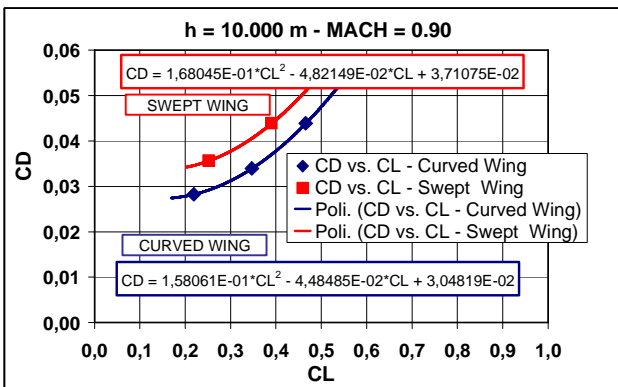


Fig. 30. Drag Polar curves (Mach=0.90)

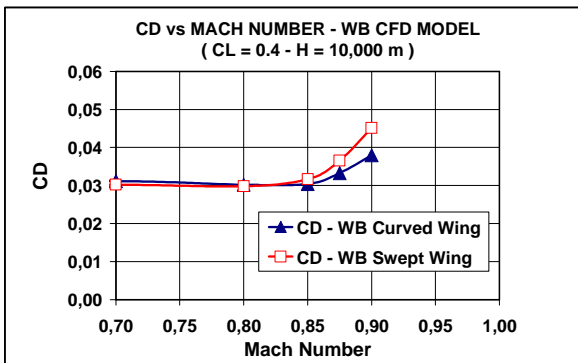


Fig. 31. CD-Mach curves (CL=0.4, Variable Lift)

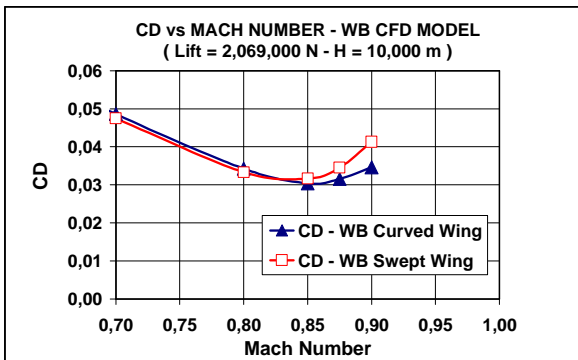


Fig. 32. CD-Mach curves (Constant Lift, Variable CL)

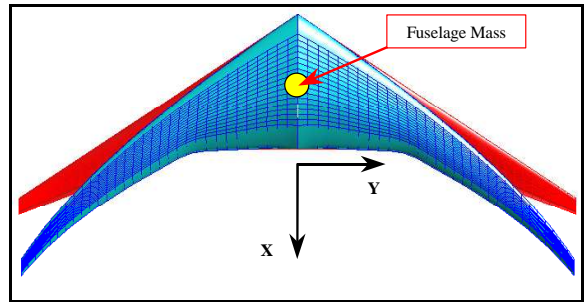


Fig. 33: FE models of the two wings (Ref. [3], Ref. [4]).

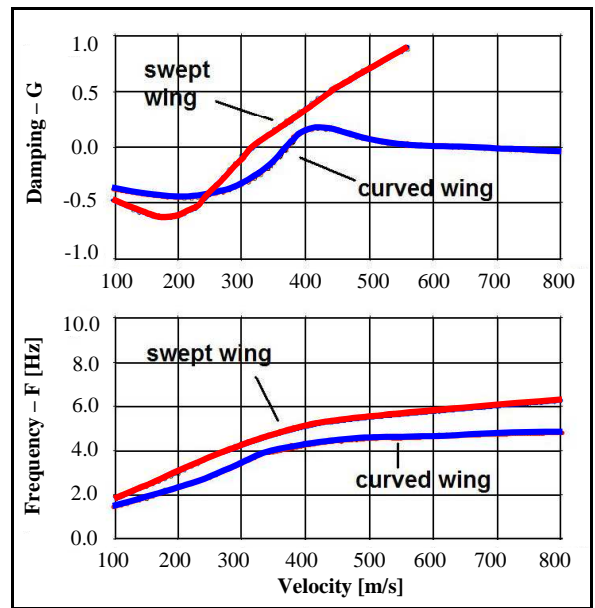


Fig. 34: Flutter condition (symmetric) - H = 0 m

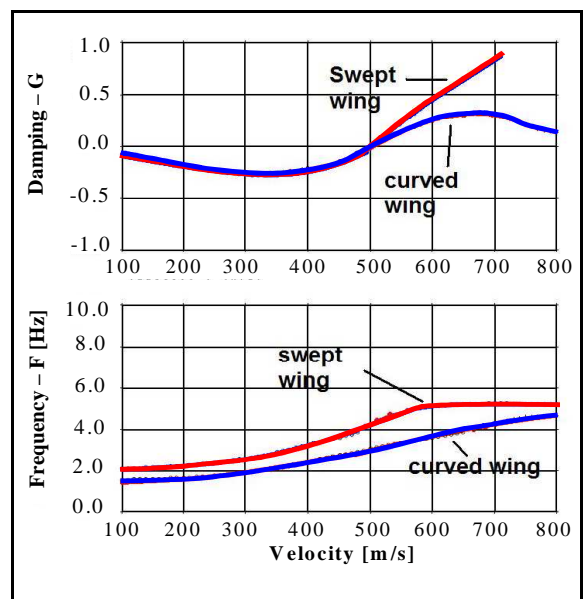


Fig. 35: Flutter condition (symmetric) - H = 10,000 m